THIRD - STAGE DEVELOPMENT OF
THE VULNERABILITY MODEL

JUNE 1977

FINAL REPORT

DDC

APR 25 1978

B
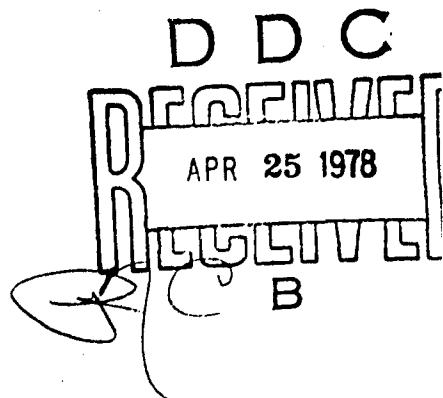
Document is available to the U.S. Public through the
National Technical Information Service,
Springfield, Virginia 22161

PREPARED FOR

U.S. DEPARTMENT OF TRANSPORTATION

UNITED STATES COAST GUARD
OFFICE OF RESEARCH AND DEVELOPMENT
WASHINGTON ,D.C. 20590

NOTICE

This document is disseminated under the sponsorship of the U. S. Department

of Transportation in the interest of information exchange. The United States

Government assumes no liability for the contents or use thereof.

The United States Government does not endorse products or manufacturers.

Trade or manufacturers' names appear herein solely because they are considered

essential to the object of this report.

1. Report No. CG-D-5-78	2. Government Accession No.	3. Recipient's Catalog No.

4. Title and Subtitle THIRD-STAGE DEVELOPMENT OF THE VULNERABILITY MODEL: A Simulation System for Assessing Damage Resulting from Marine Spills	5. Report Date June 1977
	6. Performing Organization Code

7. Author's) Andre H. Rausch, Chi K. Tsao Richard M. Rowley	8. Performing Organization Report No.

9. Performing Organization Name and Address Enviro Control, Inc. One Central Plaza 11300 Rockville Pike Rockville, Maryland 20852	10. Work Unit No. (TRAIS) 3142
	11. Contract or Grant No. DOT-CG-33377-A
	13. Type of Report and Period Covered

12. Sponsoring Agency Name and Address Department of Transportation United States Coast Guard Office of Research and Development Washington, D.C. 20590	Final Report
	14. Sponsoring Agency Code G-DSA-1/TP44

15. Supplementary Notes

The U. S. Coast Guard Office of Research and Development's technical representative for the work performed herein was DR. M. Parnarouskis.

16. Abstract

The Vulnerability Model (VM) is a computer simulation intended to provide quantitative measures of the consequences of maritime spills of hazardous materials. The simulation starts with a description of the nature of the spill itself, continues through the dispersion of the hazardous material, and then assesses the effects of resulting toxicity, fire and/or explosion, as applicable, on people and property.

This report describes the third-stage development of the VM, which consisted of improving user adaptability and applicability. This has been achieved by reducing and simplifying input requirements, by introducing new casualty summation displays, and by incorporating automatic time and demographic control characteristics into the model.

17. Key Words Vulnerability Model, Damage Assessment, Marine Spills	18. Distribution Statement Document is available to the public through the National Technical Information Service, Springfield, Virginia 22161.

19. Security Classif. (of this report) Unclassified	20. Security Classif. (of this page) Unclassified	21. No. of Pages 49	22. Price

Form DOT F 1700.7 (8-72) Reproduction of completed page authorized

CONTENTS

ACCESSION for

NTIS	White Section	☑
DDC	Buff Section	☐
UNANNOUNCED		☐
JUSTIFICATION		

BY

DISTRIBUTION/AVAILABILITY CODES

| Dist. | AVAIL. and/or SPECIAL |

A

INTRODUCTION

BACKGROUND

The Vulnerability Model (VM) is a computer simulation intended to provide quantitative measures of the consequences of maritime spills of hazardous materials. The VM is being developed for the U.S. Coast Guard under Contract D T-CG-33377-A. Its first stage of development is described in reference [1]; its second stage of development is described in reference [2]; this current report describes the latest, or third stage, development.

The VM is a research tool, one use for which is in the USCG Risk Management Program. It has been designed to treat virtually all of the large class of materials carried in bulk in marine transport. Since many of the cargoes of particular hazard are carried as bulk liquids, the VM provides useful information even in its current stage of development.

The simulation starts with a description of the nature of the spill itself, continues through the dispersion of the hazardous material, and ultimately includes assessment of the immediate effects of the spill on surrounding vulnerable resources, namely: people and property.

The VM requires three types of descriptive data that define: (1) the spill, (2) the physical setting in which the spill occurs, and (3) the vulnerable resources that are subject to the effects of the spill. The spill is described in terms of its location and spill rate, the physical and chemical properties of the spilled material, and the quantity of the spill. The physical setting is described in terms of the geometric configuration of the shoreline(s), hydrologic/oceanographic properties, and meteorological data. Vulnerable resources are described in terms of demographic distribution, property distribution, and land/water use. The geographic area of concern may represent any user-defined location, a rectangular area measuring 10 miles in length and 5 miles in width being typical of anticipated applications. The physical setting and the

---

[1] Eisenberg, N. A., C. J. Lynch, and R. J. Breeding, *Vulnerability Model: A Simulation System for Assessing Damage Resulting from Marine Spills*, CG-D-136-75, NTIS AD-A015245, prepared by Enviro Control, Inc., for the Department of Transportation, U.S. Coast Guard, June 1975.

[2] Rausch, A. H., C. J. Lynch, and N. A. Eisenberg, *Continuing Development of the Vulnerability Model: A Simulation System for Assessing Damage Resulting from Marine Spills*, Draft Final Report, prepared by Enviro Control, Inc., for the Department of Transportation, U.S. Coast Guard, February 1977.

1

distribution of vulnerable resources are described in terms of mutually exclusive geographic cells that cover the entire area of concern.

The VM operates in two phases. Phase I simulates the spill itself, the physical and chemical transformations of the spilled substance and its dissemination in space. This phase covers the time period from the initiation of the spill until a user-specified time has elapsed.

Phase I of the VM consists of submodels interconnected by an executive routine, with built-in logic dictating the sequence of submodel processing as a function of the spill development [1]. Submodels depicting spill development simulate the following phenomena: (1) cargo venting, (2) surface spreading (with or without evaporation), (3) water mixing, (4) sinking and boiling, (5) air dispersion, and (6) fire and explosion. A Time/History file of the spill sequence simulated during the first phase is retained in computer storage on magnetic tape and disk.

In Phase II the computer first matches this Time/History file to the vulnerable resources map and then assesses the effects of toxicity, explosion and/or fire on the vulnerable resources as a function of time. Estimates of deaths and nonlethal injuries to people and of damage to property are presented in computer-generated tables. A summary of the types of Phase II damage assessment is given below.

PHASE II DAMAGE ASSESSMENT

DAMAGE-CAUSING EVENT	VULNERABLE RESOURCE	TYPE OF INJURY OR DAMAGE	CAUSE OF INJURY OR DAMAGE
TOXICITY	People	Death Nonlethal Injury Irritation	Toxic Vapor: Concentration or cumulative dose
EXPLOSION	People	Death Nonlethal Injury ● Eardrum rupture ● Bone fracture ● Puncture wound ● Multiple injury	Direct Blast; Impact Direct Blast Impact Flying Fragments Two or more of the above
EXPLOSION	Structures	Structural Damage Glass Breakage	Direct Blast
POOL BURNING FIREBALL FLASH FIRE	People	Death First-Degree Burn	Thermal Radiation
POOL BURNING FIREBALL FLASH FIRE	Structures	Ignition	

2

SCOPE OF THIS WORK

The Vulnerability Work described in this report is made up of three tasks.

Task 1a -- Look Ahead

A. Define inversion and cutoff schemes on Phase I VM models so as to determine damage thresholds.

B. Compute damage assessment in Phase II of VM only in those regions where threshold hazard is exceeded.

Task 1b -- CANDO

A. Investigate feasibility of interfacing VM˙ with Defense Civil Preparedness Agency's CANDO system.

B. Apply CANDO-VM system to a selected test city.

C. If required, modify CANDO system to be congruent to VM.

Task 1c -- Explosion Damage to Structures

A. Generate explosion structural damage criteria on various classes of structures and tanks.

B. Generate probit equations for structures in (A) and include in Phase II of the VM.

Chapter 1 of this report concerns itself with Look Ahead. Chapter 2 addresses CANDO and its associated problems, while Chapter 3 enumerates and details damage data on several classes of structures not previously included in the VM.

Chapter 4 describes the toxic properties and presents resulting probit equations for hydrogen fluoride. This chemical has been added to the list of chemicals for which VM injury assessment simulations can be run.

Chapter 5 describes some simplifications made to the preparation requirements for running the VM.

CONCLUSIONS

The concrete advances made during this latest stage of VM development have been in two principal areas: VM user adaptability and VM applicability in several new and different contexts.

User adaptability itself can be and has been broken down further into an operational and an interpretive category. In the former, we have significantly eased the task of the user required to operate the VM. This has been accomplished by means of convenient and pre-prepared input schemes. On the other hand, we have expanded the latter by means of new casualty summation displays as well as automatic time and demographic controls as evidenced by "Look Ahead."

It is felt at this time that, with the exception of just a few Phase I model improvements, the thrust of a continuing program should center upon exercising the VM for all or most of the chemicals in the chemical properties file (some 900 in all) and for major U.S. Atlantic, Pacific, and Gulf ports and important inland waterways. To do so would accomplish, as an added bonus, the always desirable end of a quick-response casualty estimating system and in such a manner that it would require only minimal training to execute.

Chapter 1

LOOK AHEAD

INTRODUCTION

The former method of computing hazardous effects from air disper-
sion, fire, and explosion has been modified to exclude from considera-
tion those cells which suffer little or no ill effects from the given
marine hazard simulation. Thus, damage assessments as computed by
Phase II of the Vulnerability Model (VM) will be made only on affected
cells as predetermined by the partitioning method to be outlined for the
following Phase I subroutines:

- Fireball Model
- Pool Burning Model
- Flash Fire Model
- Plume Model of Vapor Dispersion
- Puff Model of Vapor Dispersion
- Explosion Model

Accomplishing this has involved determining critical thresholds of
the various hazards, radiation intensity, overpressure, etc., and
allowing these thresholds to control or limit the geographic extent of
VM damage assessment. This approach was determined to be more cost-
and time-effective than the purely mathematical approach of "inverting"
the presently used submodels.

FIREBALL MODEL

When a pressurized tank containing propane fails, the inside high
pressure causes the fuel to expand rapidly and mix with the ambient
air. Within a few seconds, a large cloud of highly flammable mixture
is formed. Any ignition source in the area could start a fire and
cause damage to people and material in the area. The hazard from pro-
pane burning has been studied by Hardee and Lee [3] by the use of a
fireball model. To construct this model, several important assumptions
are made.

(1) The rate of propane addition to the fireball is constant.

(2) A stoichiometric mixture is assumed to exist at ignition.

(3) All the available fuel participates in the reaction.

---

[3] Hardee, H. C., and D. O. Lee, Thermal hazard from propane fireballs,
Transp. Plann. Technol. 2:121-128, 1973.

(4) The fireball is an isothermal, homogeneous body which is spherical at all times.

(5) The fireball radiates as a blackbody.

Radiation Heat Flux

Let the radiation flux at the center of a fireball of radius, r, be q_0. Then the radiation received by a body at a distance, d $(d > r)$, from the center is given by

$$q = q_0 F_{12} \tag{1-1}$$

where

$$F_{12} = 2 \left\{ 1 - \left[1 - \left(\frac{r}{d} \right)^2 \right]^{1/2} \right\} \tag{1-2}$$

is the geometrical view factor of radiation. If τ_b is the burnout time, the total incident heat, Q, on the body is obtained by integrating equation (1-1) with time, τ,

$$Q = \int_0^{\tau_b} q_0 F_{12} \, d\tau = \frac{\tau_b}{2} \int_0^1 q_0 \left\{ 1 - \left[1 - \left(\frac{r}{d} \right)^2 \right]^{1/2} \right\} dt \tag{1-3}$$

where $t = \tau/\tau_b$ is the dimensionless time. The fireball size varies with time, and the change of its radius is expressed as

$$\frac{r}{r_b} = \left(\frac{\tau}{\tau_b} \right)^{1/3} = t^{1/3} \tag{1-4}$$

where r_b is the maximum fireball radius. Let $k = d/r_b$. Equation (1-3) can be written as

$$Q = \frac{\tau_b}{2} \int_0^1 q_0 \left\{ 1 - \left[1 - \left(\frac{r/r_b}{d/r_b} \right)^2 \right]^{1/2} \right\} dt$$

$$= \frac{\tau_b}{2} \int_0^1 q_0 \left\{ 1 - \left[1 - \frac{t^{2/3}}{k^2} \right]^{1/2} \right\} dt \tag{1-5}$$

6

The quantity q_0 depends on the air mixture and varies with time. For a first approximation, it is convenient to use the average value q_{0a} instead of q_0 and to define q_{0a} as

$$q_{0a} = \frac{Q_{k=0}}{\tau_b} \qquad (1\text{-}6)$$

The $Q_{k=0}$ has been calculated and shown in Figure 6 (in reference [3]) which can be fitted by the expression

$$Q_{k=0} = 23.35619 + 3.49189 \, (\log W_f)^3 \qquad (Btu/ft^2) \qquad (1\text{-}7)$$

where W_f is the weight of fuel burned in pounds. The values of $Q_{k=0}$ calculated from equation (1-7) are listed in Table 1-1, from which it is clear that, except at very low W_f, the approximation is appropriate. The burnout time, τ_b, is also expressed in terms of W_f as follows.

$$\tau_b = 0.6 \, (16.6385 \, W_f)^{1/6} \qquad (seconds) \qquad (1\text{-}8)$$

TABLE 1-1. TOTAL HEAT AT FIREBALL CENTER
FOR VARIOUS FUEL WEIGHTS BURNED

Weight (pounds)	Heat Input[a] (Btu/ft^2)	Heat Calculated (Btu/ft^2)
600,000	700	697
400,000	650	637
300,000	600	597
200,000	550	543
150,000	500	508
100,000	450	460
65,000	400	413
40,000	350	364
20,000	300	301
11,000	250	254
4,500	200	193
1,700	150	141
1,000	125	118
500	100	92
200	75	66
55	50	42
8	25	26
1	0	23

[a]From reference [3], Figure 6.

7

With equation (1-6), equation (1-5) is transformed to

$$q_a = \frac{q_0 a}{2} \left[1 - \int_0^1 \left(1 - \frac{t^{2/3}}{k^2} \right)^{1/2} dt \right] \tag{1-9a}$$

where

$$q_a = \frac{Q}{\tau_b} \tag{1-9b}$$

is the average heat received by the body at distance, d, from the fireball center. The integral in equation (1-9a) is evaluated as follows.

$$\int_0^1 \left(1 - \frac{t^{2/3}}{k^2} \right)^{1/2} dt$$

$$= \frac{3}{k} \left[-\frac{t^{1/3}}{4} \left(k^2 - t^{2/3} \right)^{3/2} + \frac{k^2}{8} \left(t^{1/3} \left(k^2 - t^{2/3} \right)^{1/2} + k^2 \sin^{-1} \frac{t^{1/3}}{k} \right) \right]_0^1$$

$$= \frac{3}{k} \left[-\frac{1}{4} \left(k^2 - 1 \right)^{3/2} + \frac{k^2}{8} \left(k^2 - 1 \right)^{1/2} + \frac{k^4}{8} \sin^{-1} \frac{1}{k} \right]$$

Now equation (1-9a) becomes

$$q_a = \frac{q_0 a}{2} \left\{ 1 + \frac{3}{4k} \left(k^2 - 1 \right)^{3/2} - \frac{3k}{8} \left(k^2 - 1 \right)^{1/2} - \frac{3k^3}{8} \sin^{-1} \frac{1}{k} \right\} \tag{1-10}$$

At $d = r_b$, $k = 1$ and $q_a = \frac{q_0 a}{2} \left(1 - \frac{3\pi}{16} \right)$. This is the heat flux on the surface of the fireball.

When k is much larger than unity, equation (1-10) can be expanded into a series as

$$q_a = \frac{3}{2} q_0 a \left(\frac{1}{10 \, k^2} + \frac{1}{56 \, k^4} + \dots \right) \tag{1-11}$$

It shows that the heat flux decreases very fast as the distance increases. For example, at a distance of $k = 10$, the heat flux received by a body is as small as 0.15% of that at the center.

In the Vulnerability Model, the radiation intensity for a first-degree burn is given by [1]

$$\tau I^{1.15} = 550,000 \tag{1-12}$$

where I is in Joule/m^2 sec and τ is in seconds. Substituting I for q_a in equation (1-10) and changing τ to τ_b, it yields

$$\left\{ 1 + \frac{3}{4k} \left(k^2 - 1\right)^{3/2} - \frac{3k}{8} \left(k^2 - 1\right)^{1/2} - \frac{3k^3}{8} \sin^{-1} \frac{1}{k} \right\}$$

$$= \frac{2}{q_{0a}} \left(\frac{550,000}{\tau_b} \right)^{1/1.15} \tag{1-13}$$

The problem in Look Ahead is to obtain the value of k, therefore d, for a given value of W_f. This k or d is the critical distance beyond which the people will be considered to be safe. Values on the right-hand side of equation (1-13) are computed for different values of k. The results are tabulated in Table 1-2. The data are represented by the equation

$$k = 0.1124649 + 0.533192 \left[\frac{2}{q_{0a}} \left(\frac{550,000}{\tau_b} \right)^{1/1.15} \right]^{-0.5} \tag{1-14}$$

For a given situation,

$$\left[\frac{2}{q_{0a}} \left(\frac{550,000}{\tau_b} \right)^{1/1.15} \right]$$

is computed and then k is obtained using equation (1-14). Maximum fireball radius and critical distance, d_c, are obtained as

$$r_b = 7.0 \ W_f^{1/3} \tag{1-15}$$

and

$$d_c = k \cdot r_b \tag{1-16}$$

Whenever the cell or secondary fire source distance is less than or equal to d_c, computations for the radiation intensity are performed by the subroutine FIREBL; otherwise the radiation intensity is set equal to zero. The flowchart of FIREBL is shown in Figure 1-1.

TABLE 1-2. EVALUATION OF EQUATION (1-13) FOR VARIOUS k

| $\dfrac{2 \times [550{,}000/\tau_b]^{1/1.15}}{q_{0a}}$	k
0.411	1.0
0.3070	1.1
0.2455	1.2
0.2026	1.3
0.1708	1.4
0.1463	1 5
0.1269	1.6
0.1113	1.7
0.0984	1.8
0.0877	1.9
0.0787	2.0
0.0710	2.1
0.0644	2.2
0.0587	2.3
0.0538	2.4
0.0494	2.5
0.0456	2.6
0.0422	2.7
0.0392	2.8
0.0364	2.9
0.0340	3.0
0.0318	3.1
0.0298	3.2
0.0280	3.3
0.0264	3.4
0.0248	3.5
0.0235	3.6
0.0222	3.7
0.0210	3.8
0.0200	3.9
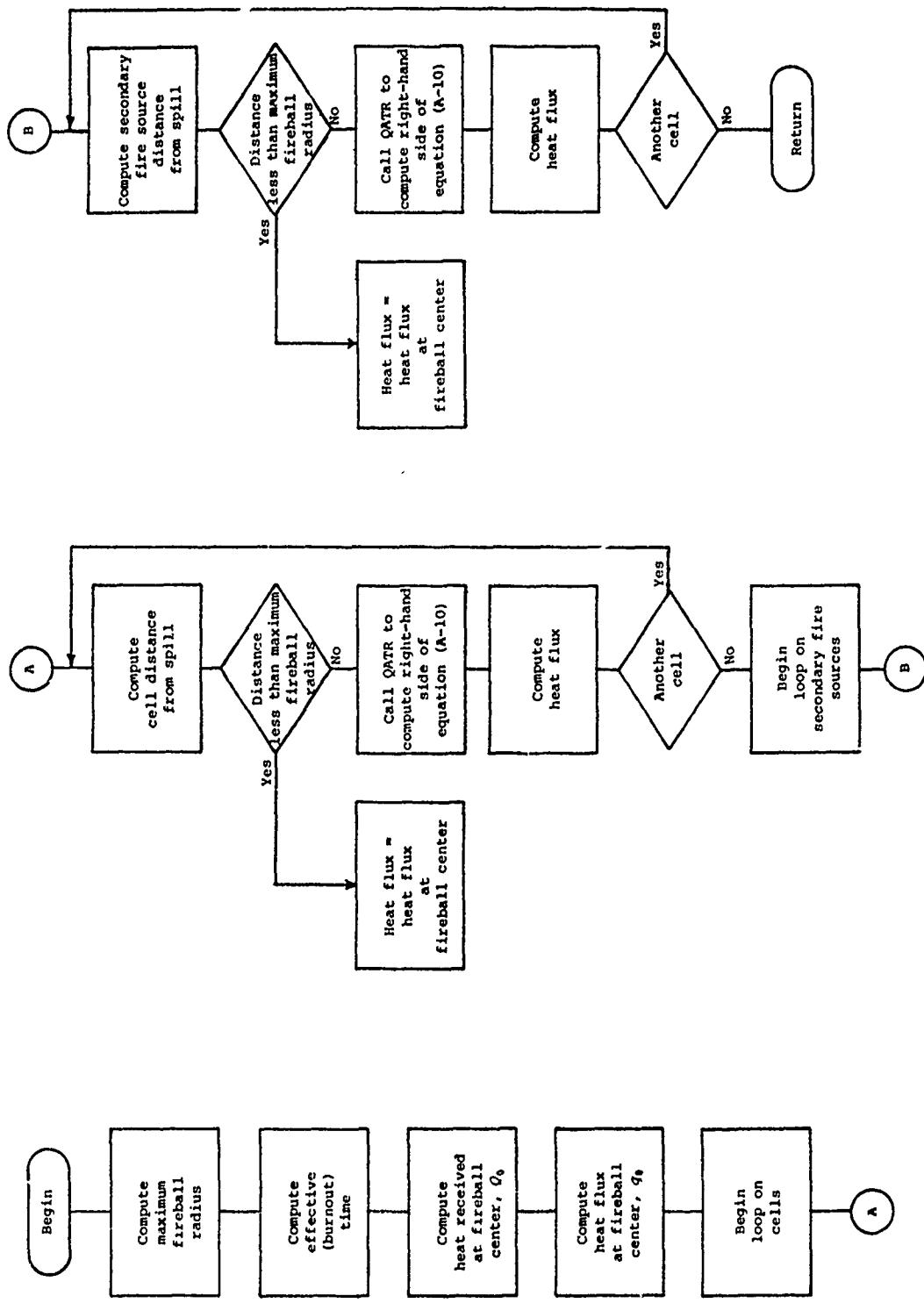
FIGURE 1-1. Flowchart for Subroutine FIREBL

11

POOL BURNING MODEL

The subroutine PLBURN calculates the radiation intensity at various cells and secondary fire sources in the event of pool burning. This subroutine has been modified, so as to limit the computations for the radiation intensity to only those cells and secondary fire sources where the level of radiation intensity is high enough to cause at least a first-degree burn. First-degree burns constitute the Look Ahead criterion for this case.

The radiation intensity for the first-degree burn is given by [1]

$$t \, I^{1.15} = 550,000$$

where I is in Joule/m^2 sec and t is in seconds.

Assuming the transmissivity of medium, the emissivity of flame, and the absorptivity of the receptor each equal unity, we have

$$I = F \sigma T^4$$

where

    F = view factor of receptor to flame

    σ = Stefan-Boltzmann constant

    T = absolute temperature of flame

That is,

$$F = \frac{I}{\sigma T^4} = \frac{[550,000/t]^{1/1.15}}{\sigma T^4} \qquad (1\text{-}17)$$

for the radiation intensity to cause a first-degree burn.

The view factor for the cylindrical flame is a function of:
    (1) flame diameter,
    (2) flame height,
    (3) flame angle, and
    (4) distance of receptor (differential vertical plane) from flame center.

It is assumed in the subroutine SVEIW that the receptor is located at a downwind position and thus gives the maximum view factor for the given distance under otherwise identical conditions. The subroutine SVEIW

calculates the view factor for the given flame diameter, flame angle, flame height, and the distance of the receptor from the flame center. However, our problem is to obtain the distance of receptor from flame center for the given flame diameter, flame height, flame angle, and view factor. That is, we need to invert the subroutine SVEIW. This is accomplished in the following manner.

The function FCT2(S) calculates the following for any given value of receptor distance from flame center, S:

(view factor calculated by SVEIW) — (F given by equation (1-17))

Various values of S are passed to the function subprogram by the subroutine RTMI until the above calculation = 0; i.e., the view factor calculated by SVEIW for this S = F given by equation (1-17).

This value of S is named XMAX in the subroutine PLBURN. It has been found that XMAX will be less than $50 \times R$, where R is the radius of the flame. Therefore, the subroutine RTMI looks for XMAX in the range of distance lying between 1.01*R and 50.0*R.

This value of XMAX is multiplied by a safety factor of 1.1 to obtain DISMAX. Whenever the cell or secondary fire source distance is less than or equal to DISMAX, computations for the radiation intensity are performed by the subroutine PLBURN; otherwise, radiation intensity is set equal to 0.0. This way, a considerable saving in computer time is realized.

FLASH FIRE MODEL

The subroutine FLFIRE calculates the radiation at various cells and secondary fire sources in the event of a flash fire. This subroutine has been modified so as to limit the computations for the radiation intensity to only those cells and secondary fire sources where the level of radiation intensity is high enough to cause at least a first-degree burn.

The radiation intensity for the first-degree burn is given by [1]

$$t\, I^{1.15} = 550,000$$

The subroutine FLFIRE calculates the radiation intensity according to the equation

$$I = F_{12}\, \sigma\, [T_{eff}{}^4 - T_a{}^4] \tag{1-18}$$

13

where

$$T_{eff} = \frac{1}{2} \text{[initial flame temperature + air temperature]}$$

$$\sigma = \text{Stefan-Boltzmann constant}$$

$$F_{12} = \text{view factor}$$

$$= \frac{1}{2} H^2 \quad \text{where}$$

$$H = \frac{r}{\ell} = \frac{\text{radius of flash fire}}{\text{distance from fire center to cell center}}$$

Equation (1-18) can be rewritten as

$$I = \frac{r^2}{2\ell^2} \sigma [T_{eff}^4 - T_a^4] \tag{1-19}$$

The effective duration of a flash fire is taken to be $3\, t_{1/2}$. The problem in Look Ahead is to obtain the value of ℓ for the given value of $I = [550,000/3\, t_{1/2}]^{1/1.15}$. Therefore, we have from equation (1-19)

$$\left[\frac{550,000}{3\, t_{1/2}}\right]^{1/1.15} = \frac{r^2}{2\ell^2} \sigma \left[T_{eff}^4 - T_a^4\right]$$

or

$$\ell = \left[\frac{r^2 \sigma \left(T_{eff}^4 - T_a^4\right)}{2\left(\frac{550,000}{3\, t_{1/2}}\right)^{1/1.15}}\right]^{0.5}$$

This value of ℓ is named DISMAX in the subroutine FLFIRE. Whenever the cell or secondary fire source distance is less than or equal to DISMAX, computations for the radiation intensity are performed by the subroutine FLFIRE; otherwise the radiation intensity is set equal to 0.0. Thus, a saving in computer time is effected.

14

PLUME MODEL OF VAPOR DISPERSION

The subroutine VAPCCS calculates vapor dispersion for the plume model. This subroutine has been modified so as to limit the computations for vapor dispersion to only those cells where the level of vapor concentration is high enough to be combustible.

The vapor concentration C at some point (x,y,z) at time t for the plume model is given by equation (1-20).

$$C(x,y,z,t) = \frac{2\,Q}{(2\pi)\,U\,\sigma_y\,\sigma_z}\ \exp\left[-\frac{y^2}{2\,\sigma_y^2} - \frac{z^2}{2\,\sigma_z^2}\right] \qquad (1\text{-}20)$$

$$\text{for } 0 \leqslant t_v \leqslant t_e$$

and

$$C(x,y,z,t) = 0 \quad \text{for } t_v < 0 \text{ and } t_v > t_e \qquad (1\text{-}21)$$

where

Q = rate of vapor liberation (kg/s)

U = wind speed (m)

σ_y, σ_z = dispersion coefficient (m)

t_e = time at which the gas venting or evaporating is complete

$t_v = t - x/U$ = time at which the cargo vapor is observed at x,y,z .

The dispersion coefficients, σ_y and σ_z, are functions of x distance and are evaluated at an imaginary distance, $x' = x + 5\,d$, where d is the diameter of the pool.

Let $C = C_S$ = a specified vapor concentration which is the lower limit of flammability or the irritation threshold for the vapor. Then from equation (1-20) it follows that

$$\frac{y^2}{\sigma_y^2} + \frac{z^2}{\sigma_z^2} = 2\,\ell n\left[\frac{Q}{\pi\,U\,\sigma_y\,\sigma_z\,C_S}\right]$$

On the ground $z = 0$, and equation (1-21) becomes

$$y^2 = 2\,\sigma_y^2\,\ell n\left[\frac{Q}{\pi\,U\,\sigma_y\,\sigma_z\,C_S}\right]$$

Recall that σ_y and σ_z are functions of x, so that y^2 is also a function of x. All cells outside the curve $y^2 = f(x)$ have vapor concentrations less than the lower limit of C_s. In general, for any cell with center at (x_c, y_c, z_c), if

$$t > t_e + \frac{x_c}{U}$$

or

$$t < \frac{x_c}{U}$$

or

$$y_c^2 > 2\sigma_y^2 \; \ln\left[\frac{Q}{\pi U \sigma_y \sigma_z C_s}\right]$$

a zero vapor concentration will be assigned to the cell.

PUFF MODEL OF VAPOR DISPERSION

The subroutine VAPCIS calculates vapor dispersion for the puff model. This subroutine has been modified so as to limit the computations for vapor dispersion to only those cells where the level of concentration is above that for irritation and combustion.

The vapor concentration C at a point (x, y, z) far from the center of spilling of the puff model is given by

$$C(x,y,z,t) = \frac{m}{(2\pi)^{3/2} \sigma_x \sigma_y \sigma_z} \; exp\left[-\frac{(x - Ut)^2}{2\sigma_x^2} - \frac{y^2}{2\sigma_y^2}\right]$$

$$\left\{ exp\left[-\frac{(z - H)^2}{2\sigma_z^2}\right] + exp\left[-\frac{(z + H)^2}{2\sigma_z^2}\right]\right\} \tag{1-22}$$

where

m = mass of vapor liberated (kg)

$\sigma_x, \sigma_y, \sigma_z$ = dispersion coefficients (m)

U = wind speed (m/sec)

16

Let C_S be a specified vapor concentration which equals the lower limit of flammability or the irritation threshold for the vapor. With $C = C_S$ equation (1-22) is written as:

$$\exp\left[-\frac{(x - Ut)^2}{2\sigma_x^2} - \frac{y^2}{2\sigma_y^2}\right]\left\{\exp\left[-\frac{(z - H)^2}{2\sigma_z^2}\right] + \exp\left[-\frac{(z + H)^2}{2\sigma_z^2}\right]\right\}$$

$$= \frac{(2\pi)^{3/2}\,\sigma_x\,\sigma_y\,\sigma_z\,C_S}{m} \qquad (1-23)$$

The constant vapor concentration profile is an ellipsoid. If for a cell with center at (x_C, y_C, z_C), the inequality

$$\exp\left[-\frac{(x_C - Ut)^2}{2\sigma_x^2} - \frac{y_C^2}{2\sigma_y^2}\right]\left\{\exp\left[-\frac{(z_C - H)^2}{2\sigma_z^2}\right] + \exp\left[-\frac{(z_C + H)^2}{2\sigma_z^2}\right]\right\}$$

$$< \frac{(2\pi)^{3/2}\,\sigma_x\,\sigma_y\,\sigma_z\,C_S}{m} \qquad (1-24)$$

holds, the cell is considered to be safe and the vapor concentration at the cell is assumed to be zero.

For locations near the center of the spill, the concentration is calculated as follows. At the center of the puff, the concentration is

$$C_0 = \frac{2m}{(2\pi)^{3/2}\,\sigma_x\,\sigma_y\,\sigma_z} \qquad (1-25)$$

If C_0 is greater than C_p, the density of the pure cargo vapor at ambient atmospheric pressure and temperature, then the concentration at the point (x, y, z) will be

$$C = C_p \qquad \text{when} \quad r' < R'$$

$$C = C_p \exp\left(-\frac{(r' - R')^2}{2}\right) \qquad \text{when} \quad r' > R' \qquad (1-26)$$

where

$$r' = \left[\frac{(x - Ut)^2}{\sigma_x^2} + \frac{y^2}{\sigma_y^2} + \frac{z^2}{\sigma_z^2}\right]^{1/2} \qquad (1-27)$$

17

and R' is the root of the cubic equation (reference [1], pp. 189-190).

$$R'^3 + P R'^2 + Q R' + S = 0 \qquad (1-28)$$

and

$$P = \frac{3}{2} (2\pi)^{1/2}$$

$$Q = 6$$

$$S = P - \frac{3\,m}{2\,\pi\,C_p\,\sigma_x\,\sigma_y\,\sigma_z}$$

With equation (1-27) and $C = C_s$, equation (1-26) can be written as

$$\left[\left(\frac{x - Ut}{\sigma_x}\right)^2 + \left(\frac{y}{\sigma_y}\right)^2 + \left(\frac{z}{\sigma_z}\right)^2\right]^{1/2} = R' + \sqrt{2\,\ln\left(\frac{C_p}{C_s}\right)} \qquad (1-29)$$

Hence for any cell at (x_c, y_c, z_c), if the inequality

$$\left[\left(\frac{x_c - Ut}{\sigma_x}\right)^2 + \left(\frac{y_c}{\sigma_y}\right)^2 + \left(\frac{z_c}{\sigma_z}\right)^2\right]^{1/2} > R' + \sqrt{2\,\ln\left(\frac{C_p}{C_s}\right)}$$

holds, the vapor concentration at the cell is assumed to be zero.

EXPLOSION MODEL

The subroutine EXPLOD computes the peak overpressure and the heat released due to gas explosion. This subroutine has been modified so as to limit the computations for explosion to only those cells where the overpressure or heat produced due to explosion exceeds certain lower limits.

The energy yield in a gas explosion is given by the equation

$$W = (-\Delta H)\,\frac{m_e}{M} \qquad \text{(kcal)} \qquad (1-30)$$

18

where

ΔH = heat of combustion   (kcal/kg mol)

m_e = mass of exploding fuel   (kg)

M = molecular weight of the fuel

The damage assessment due to explosion is calculated from the scaling laws which are stated as follows (reference [1], p. 55):

$$d_S = \frac{d_a \, (P/P_0)^{1/3}}{(W'/W_0)^{1/3} \, (T/T_0)^{1/3}} \tag{1-31}$$

$$t_a = \frac{t_S \, (W'/W_0)^{1/3}}{(P/P_0)^{1/3} \, (T/T_0)^{1/6}} \tag{1-32}$$

$$I_a = \frac{I_S \, (W'/W_0)^{1/3} \, (P/P_0)^{2/3}}{(T/T_0)^{1/6}} \tag{1-33}$$

where

d_S = scaled distance from explosion center   (m)

d_a = actual distance from explosion center   (m)

P,T = pressure and temperature of the atmosphere in the actual case (bar, °K)

P_0,T_0 = pressure and temperature of the atmosphere in the case of the reference explosion ($P_0 = 1$ bar, $T_0 = 288.15$°K)

W' = effective energy yield of the actual explosion

W_0 = energy yield of the reference explosion (1 kg TNT yields 1.12×10^6 calories; thus, $W_0 = 1.12 \times 10^6$ calories)

t_a = actual time (s)

t_S = scaled time (s)

I_a = actual impulse (N·s/m^2)

I_S = scaled impulse (N·s/m^2)

For an explosion with a center on a rigid surface, the surface reflects completely all explosive energy impinging upon it. If the ground can be considered as a rigid surface, then the effective energy yield W'

will be twice that of the explosive energy yield, or $W' = 2W$. The data for a reference spherically symmetrical explosion are stored in the computer. If the critical impulse for body injury is determined then from equation (1-30) and equations (1-31), (1-32), and (1-33) and the reference data, the critical distance for a certain explosive mass can be obtained from equations (1-30) through (1-33) and the reference data. The procedure is: (a) compute W from equation (1-30) and $W' = 2W$; (b) calculate I_S from equation (1-33) for the given critical impulse I_a; (c) from reference data find scaled distance d_S corresponding to the I_S; then (d) from equation (1-31) compute the actual distance d_a.

From experiment, it is found that for whole body safety the critical impulse is

$$I_p = 283.8 \text{ N}\cdot\text{s/m}^2$$

This value will be used for the critical impulse.

Chapter 2

ADDITIONAL DATA BASE CREATION/ACCESS SYSTEMS

This task was directed toward determining whether a more efficient method of geographic data base compilation and more precise damage assessment could increase the usability and accuracy of the VM. One of the prime candidates for this data base and access system is the CANDO system used in conjunction with the Geographic Base File (GBF) as now implemented at the Defense Civil Preparedness Agency (DCPA). The CANDO system was designed by the DCPA to allow a user familiar with a geographic location to assess vulnerable resources within a specific area by outlining that area with intersecting street names. The CANDO software accesses the GBFs and presents the data to the user, either graphically or on hard copy medium.

Because the thrust of present work on the VM is toward a more user-oriented system, with less emphasis on user familiarity with the VM's internal structure, any improvements to the VM must reflect this requirement. From a thorough analysis of the VM requirements along with the detailed requirements of the CANDO system, we have made the following determinations.

- The GBFs contain more detailed vulnerable resources data than our geographic files and, in an ideal situation, would allow much greater resolution of damage than our files. Vulnerable resources data in the GBFs are detailed on a street intersection-to-intersection basis. However, the GBFs for the majority of the U.S. cities contain numerous errors, and to this date only a handful of cities have completed and corrected GBFs. These errors in street designation and location were introduced mainly because of a lack of standardization and consistency in procedure by the cities compiling these data. The error detection process is extremely slow and involves plotting an entire city from the GBF and overlaying it with a correct grid system. An added difficulty is that the GBFs are much larger than our geographic file, thus causing an increase in both the access time and the computation time needed to perform damage assessment on vulnerable resources. Finally, it was discovered that none of the cities with a complete GBF contains a port. Until the GBFs for strategic ports are complete, these files are of no value to the VM.

- The CANDO software system was not designed for a user-oriented system such as the VM. In order for CANDO to be effective, the user must be familiar with the geographic distribution of streets and other boundary lines. Not only is this not consistent with the development of a user-oriented VM, but it requires far too much knowledge of the geographic area to be useful. The definition of boundary lines must be done by defining four streets or lines which form a rectangle. Any unclosed system will result in incorrect execution or in nonexecution. The VM now defines a damage contour and assesses damage only within this contour, thus it is not necessary for CANDO also to define this boundary.

- Precision of CANDO is superior to the precision of the VM. This is because the respective research goals of each program are different. Because system precision of a linked CANDO-VM is defined by the component with lowest precision if the components are independent, one buys no further increase in accuracy by including CANDO.

In order to circumvent some of the difficulties posed by the use of CANDO, ECI investigated the use of alternative levels of GBFs. A meeting was held of ECI, USCG, and Bureau of the Census personnel. Based on the results of this meeting, it was determined that the geographic resources data base most suitable to the needs of the VM is the Master Enumeration District List X (MEDLX). The MEDLX was created by the Bureau of the Census to (1) join the names of counties, minor civil divisions (MCDs) or census county divisions (CCDs) and places with the geographic codes specific to each, and (2) assign small area population and housing unit counts with the geographic codes and area names. The MEDLX provides all of the census geographic codes for each state, county, MCD or CCD, MCD (or CCD) place segment, census tract, enumeration district (ED), and block group. The total population and housing unit count is provided for each area in the list. In addition, the longitude and latitude of the center of each block group (two to nine block groups per tract) is provided. This file contains some errors in centroid locations; however, these errors would be readily visible and correctable by inspection. The files are contained on five magnetic tapes, each tape having data for one or two geographic regions (nine regions in the U.S.). The software program to access these tapes has been written by ECI and will require only minor modifications for future execution. Using MEDLX will eliminate the manual preparation of geographic resources data for the VM, which takes approximately 30 hours per city. The only disadvantage in using the data on these tapes is that average housing value, used in Phase II of the VM, is not included. This disadvantage will be overcome by adding average housing value to the MEDLX tapes by manually transferring the housing data from block census reports for those cities of interest. This will require approximately four hours per city.

22

Chapter 3

EXPLOSION DAMAGE TO STRUCTURES

INTRODUCTION

Damage criteria have been generated for several structural cate-
gories subjected to explosion effects. Various classifications, span-
ning the range from industrial warehouses to spherical petroleum tanks,
have been examined and subjected to probit analysis for insertion in
Phase II of the Vulnerability Model (VM). The data source for the new
addition was the National Fallout Shelter Survey (NFSS) classification
[4,5]. While other sources of damage assessment criteria were examined
and evaluated, none contained the degree of information required to give
results consistent with other Phase II damage assessment procedures,
such as in the case of fire [6,7].

EXPLOSION DAMAGE

The blast wave resulting from a vapor-phase explosion is quite a
different matter from that resulting from a condensed-phase or nuclear
explosion. Yet the assumption that vapor- and condensed-phase explo-
sions yield similar results leads to relatively small errors. Because
much of the damage assessment analysis is presented in terms of basic blast
wave parameters, such as overpressure, if the data become available to
predict the behavior of diffuse explosions, these predicted values may
be used with the preexisting data to provide a more accurate damage
assessment. In the absence of a convincing and complete analysis of
diffuse explosions, the approach has been and will be to treat the dif-
fuse explosions as condensed-phase explosions and to assess damage
accordingly. This approach is consistent with the state of the art and
with assumptions made elsewhere in the VM [1, ch. 4].

---

[4] Wiehle, C. K., and J. L. Bockholt, *Blast Response of Five NFSS
    Buildings,* Stanford Research Institute (SRI), Menlo Park, Calif.,
    October 1971.

[5] Wiehle, C. K., and J. L. Bockholt, *Existing Structures Evaluation,
    Part V: Applications,* Stanford Research Institute, Menlo Park,
    Calif., July 1971.

[6] Fugelso, L. E., L. M. Weiner, and T. H. Schiffman, *Explosion Effects
    Computation Aids,* GARD Project No. 1540, General American Research
    Division, General American Transportation Corp., Niles, Ill., June
    1972 (AD-903279L).

[7] Glasstone, S. (ed.), *The Effects of Nuclear Weapons,* U.S. Atomic
    Energy Commission, April 1962.

DAMAGE TO STRUCTURES

To begin the discussion of explosion damage to structures, it is necessary to consider the nature of the interaction between an explosive shock and a structure [8,9].

Damage to a structure from blast shocks comes from the dynamic response of the structure to forces caused by the blast wave. An analytic solution for the resulting composite structural motions would come from a solution of the equation of motion, an equation with many degrees of freedom and one in which a tractable solution--even in numerical form--would be very difficult to perform. An equation of this type would have three kinds of terms: an inertial term representing the acceleration of a given degree of freedom; a potential term representing the structural resistance of the building; and a source term representing the blast wave. The functional nature of the source term, the blast wave, is known or can be computed. A similar statement can be made for the inertial terms, which are simply second-order time derivatives of the displacements of each degree of freedom. The same cannot be said for the structural potential of the building itself, since we have no way of generalizing the structural features and parameters of even one class of buildings so as to allow their insertion into a potential function.

From all that has been said thus far, it is not surprising that only a few numerical solutions to the equation of motion for structural response have been made.

As an alternative to numerical solutions for structural motion, various empirical estimates of the damage potential of blast have been used. The most common of these is based on the peak overpressure in the free-field blast wave. For example, it is usually stated that a peak overpressure of such-and-such psi causes major structural damage. Such a statement is, of course, a crude approximation since it ignores one of the two parameters necessary to specify a blast damage uniquely, the second one being structural response. Although details of the structural response could be considered, especially for singularly important buildings, for the present it is more cost-effective to characterize a blast wave-structural response problem by the blast overpressure alone.

The Defense Civil Preparedness Agency has developed a procedure for the evaluation of existing structures subjected to nuclear air blast. The objective of their overall research program was to develop an evaluation procedure for determining the blast protection afforded by existing fallout shelter structures and private residences.

---

[8] Kinney, G. F., *Engineering Elements of Explosions,* NWC TP-4654, Naval Weapons Center, November 1968.

[9] Kinney, G. F., *Explosive Shocks in Air,* The Macmillan Co., New York, 1962.

This effort was of two basic kinds. The earliest efforts in the NFSS program [4,5] had been concerned with the visual and physical examination of exterior walls, window glass, steel frame connections, ceiling construction and their applications. In short, the earlier approach could be called an empirical one. Subsequent to this, however, a probabilistic approach to air blast failure was undertaken for urban structures [10]. Finally, comprehensive summaries were given [11,12] along with an interesting summary of the dynamic analysis of a typical building [13]. This collection of works defines the state of the art of structural blast response.

While the amount of work and analytical data generation is impressive, very little concrete experimental data on a given structure in toto exist to firmly back the estimates and projections made in the aforementioned studies. For this reason, we have chosen the studies carried out in Detroit [4] and Greensboro [5] as a prototype data source base, because estimates of structural collapse overpressure were based largely on visual inspection of construction features and architects' drawings. This generally resulted in two sets of figures, those from visual inspection yielding the lower destruction overpressure. We briefly summarize the methods used in the Detroit and Greensboro studies.

As part of an integrated program to create a survey method for air blast effects, an initial field survey was made in 1970 of several preselected NFSS buildings in Detroit, Michigan, and Greensboro, North Carolina. The survey was carried out mainly to obtain a complete structural description of the buildings that would be adequate for building-damage prediction purposes. Essentially, two analyses were made of each building studied: the first used data obtained from the on-site inspection of the building; while the second analysis used data from the actual building plans. It was hoped that such a procedure would provide a cross-check on the accuracy of the survey technique.

[10] Pickering, E. E., and J. L. Bockholt, *Probabilistic Air Blast Failure Criteria for Urban Structures,* Stanford Research Institute (for Office of Civil Defense), Menlo Park, Calif., November 1971.

[11] Wiehle, C. K., *All Effects Shelter Survey System -- Summary of Dynamic Analyses of 25 NFSS Buildings,* Stanford Research Institute (for Defense Civil Preparedness Agency), Menlo Park, Calif., March 1973.

[12] Wiehle, C. K., *Summary of the Dynamic Analyses of the Exterior Walls and Floor Systems of 50 NFSS Buildings,* Stanford Research Institute (for Defense Civil Preparedness Agency), Menlo Park, Calif., June 1974.

[13] Wiehle, C. K., *Dynamic Analysis of a Building and Building Elements,* Stanford Research Institute (for Defense Civil Preparedness Agency), Menlo Park, Calif., April 1974.

The predictions of the collapse overpressure of the buildings were based on analysis of the exterior walls using the procedures in references [14] and [15]. An explicit assumption made in the analysis was that the exterior walls always fail before the structural frame. Thus failure implies collapse or disintegration of the wall.

As noted earlier, the load time function on a wall in an actual building subjected to nuclear blast is a complex phenomenon, and thus a precise description of such a loading function and the overpressure history are not too meaningful in making collapse predictions. Therefore, the predicted collapse overpressures used in constructing the probit equations for various structures given here are the peak incident overpressures of the free-field blast wave that result in wall failure. In general, where there was divergence between the peak pressures predicted from the on-site survey and building plans, the former were chosen since they alone represented the physical reality of the building in question and thus came closest to being "experimental" results.

A few words should be said about detonation damage to industrial tankage. To quote Stephens [16] on the high vulnerability of industrial tankage:

> The blast resistance of tanks is low; in fact, a nuclear air blast of a 1 megaton weapon detonated at optimum height 4-1/2 miles away would damage most tank installations. Blast resistance of a typical cone roof tank has been calculated to be only 0.5 psi (dynamic) or less, and ladders on tanks become flying missiles at 10 psi overpressure. A full tank is less susceptible to damage than an empty one, but for damage assessment problems, it is...assumed that all tanks are half full.
>
> Cone roof tanks commonly used for oil storage are designed for a live load of 25 pounds per square *foot* with an allowable stress of 18,000 psi. The ultimate strength of the material of 55,000 psi

[14] Wiehle, C. K., and J. L. Bockholt, *Existing Structures Evaluation, Part I: Walls,* Stanford Research Institute (for Office of Civil Defense), Menlo Park, Calif., November 1968 (AD-687 293).

[15] Wiehle, C. K., and J. L. Bockholt, *Existing Structures Evaluation, Part IV: Two-Way Action Walls,* Stanford Research Institute (for Office of Civil Defense), Menlo Park, Calif., September 1970 (AD-719 306).

[16] Stephens, M. M., *Vulnerability of Total Petroleum Systems,* DAHC20-70-C-0216, Defense Civil Preparedness Agency, Work Unit 4362A, May 1973.

would require about 75 pounds per square foot to cause failure or about 0.5 psi.

Floating roof tanks of the pontoon type can stand up to 20 psi overpressure. Danger exists, however, from flying steel which may penetrate the side walls of even a relatively strong tank.

DAMAGE LEVELS AND PROBIT EQUATIONS

The damage levels for structures and tanks are given in Tables 3-1 through 3-11. To obtain the probit equation for glass breakage, it was assumed that the 10% level for structural damage corresponds to the 90% level for glass breakage. The probit equations for damage to structures from explosion are thereby obtained. All results of Table 3-1 through 3-11 are stored in Phase II of the VM for damage assessment.

In each of the following probit equations, the peak overpressure, P, is measured in N/m^2.

TABLE 3-1. EXPLOSION DAMAGE LEVELS FOR FRAME STRUCTURES*

Target	Damage Level	Peak Overpressure	
		psi	(N/m^2)
Frame structure, wood, brick, masonry private homes	Threshold Glass Breakage (1%)	0.25	1,724
	Threshold Structural Damage (1%)	0.90	6,200
	50% Structural Damage	3.00	20,700
	Total Damage (99%)	5.00	34,500

*Relationship between structural damage and peak overpressure. Based on data from reference [5] for frame structures exposed to a blast from an explosion of 500 tons TNT-equivalent yield.

Probit Equations
Glass Breakage Probit = $-12.6 + 2.1$ $\ln P$
Structural Damage Probit = $-20.0 + 2.6$ $\ln P$

TABLE 3-2. EXPLOSION DAMAGE LEVELS FOR PUBLIC LIBRARY*

Target	Damage Level	Peak Overpressure	
		psi	(N/m^2)
Reinforced concrete frame, brick veneer, two-story public library	Threshold Glass Breakage (1%)	0.25	1,724
	(10%) Structural Damage	4.10	28,269
	(90%) Structural Damage	7.9	54,469

*Relationship between structural damage and peak overpressure. Based on data from reference [4], page 16.

Probit Equations

Glass Breakage Probit $= -6.9 + 1.3 \, \ln P$

Structural Damage Probit $= -36.3 + 3.9 \, \ln P$

TABLE 3-3. EXPLOSION DAMAGE LEVELS FOR TWO-STORY DORMITORY*

Target	Damage Level	Peak Overpressure	
		psi	(N/m^2)
Structural steel frame; load-bearing exterior wall, nonreinforced masonry, two-story dormitory	Threshold Glass Breakage (1%)	0.25	1,724
	(10%) Structural Damage	6.9	47,574
	(90%) Structural Damage	8.6	59,295

*Based on data from reference [4], page 40.

Probit Equations

Glass Breakage Probit $= -5.4 + 1.09 \, \ln P$

Structural Damage Probit $= -121.5 + 11.6 \, \ln P$

TABLE 3-4. EXPLOSION DAMAGE LEVELS FOR LOW OFFICE BUILDING*

Target	Damage Level	Peak Overpressure	
		psi	(N/m^2)
Structural steel frame, brick and granite veneer, brick backing, low office building	Threshold Glass Breakage (1%)	0.25	1,724
	(10%) Structural Damage	3.0	20,684
	(90%) Structural Damage	4.8	33,095

*Based on data from reference [4], page 44.

Probit Equations

Glass Breakage Probit $= -8.16 + 1.45 \ln P$

Structural Damage Probit $= -50.4 + 5.4 \ln P$

TABLE 3-5. EXPLOSION DAMAGE LEVELS FOR TEN-STORY APARTMENT BUILDING*

Target	Damage Level	Peak Overpressure	
		psi	(N/m^2)
Structural steel frame, brick veneer/unreinforced concrete block wall, ten-story apartment building, 100 ft high	Threshold Glass Breakage (1%)	0.25	1,724
	(10%) Structural Damage	1.7	11,721
	(90%) Structural Damage	3.8	26,200

*Based on data from reference [4], page 26.

Probit Equations

Glass Breakage Probit $= -11.37 + 1.88 \ln P$

Structural Damage Probit $= -26.1 + 3.18 \ln P$

TABLE 3-6. EXPLOSION DAMAGE LEVELS FOR TEN-STORY FACTORY*

Target	Damage Level	Peak Overpressure	
		psi	(N/m^2)
Structural steel frame, reinforced concrete structure, ten-story factory, 150 ft high	Threshold Glass Breakage (1%)	0.25	1,724
	(10%) Structural Damage	0.9	6,205
	(90%) Structural Damage	2.4	16,547

*Based on data from reference [4], page 10.

Probit Equations
Glass Breakage Probit = -18.3 + 2.8 $\ln P$
Structural Damage Probit = -19.1 + 2.6 $\ln P$

TABLE 3-7. EXPLOSION DAMAGE LEVELS FOR SERVICE WAREHOUSE*

Target	Damage Level	Peak Overpressure	
		psi	(N/m^2)
Reinforced concrete frame, floors, and walls, five-story service warehouse	Threshold Glass Breakage (1%)	0.25	1,724
	(10%) Structural Damage	19.4	133,758
	(90%) Structural Damage	20.4	140,653

*Based on data from reference [5], page 47.

Probit Equations
Glass Breakage Probit = -3.5 + 0.83 $\ln P$
Structural Damage Probit = -59.5 + 50.9 $\ln P$

TABLE 3-8. EXPLOSION DAMAGE LEVELS FOR DEPARTMENT STORE*

Target	Damage Level	Peak Overpressure	
		psi	(N/m^2)
Steel frame, concrete floor, brick facing unreinforced, department store	Threshold Glass Breakage (1%)	0.25	1,724
	(10%) Structural Damage	0.50	3,447
	(90%) Structural Damage	0.70	4,826·

*Based on data from reference [5], page 25.

Probit Equations

Glass Breakage Probit $= -36.2 + 5.2 \ln P$

Structural Damage Probit $= -58.3 + 7.6 \ln P$

TABLE 3-9. EXPLOSION DAMAGE LEVELS FOR FLOATING-ROOF TANK*

Target	Damage Level	Peak Overpressure	
		psi	(N/m^2)
Steel petroleum tank, floating roof	(20%) Structural Damage	3.5	24,132
	(99%) Total Destruction	20.0	137,895

*Based on data from reference [10], page 145.

Probit Equation

Total Destruction Probit $= -14.2 + 1.8 \ln P$

TABLE 3-10. EXPLOSION DAMAGE LEVELS FOR VERTICAL PRESSURE VESSEL*

Target	Damage Level	Peak Overpressure	
		psi	(N/m^2)
Steel, right circular cylinder, vertical pressure vessel	(20%) Structural Damage.	12.0	82,737
	(99%) Total Destruction	14.0	96,527

*Based on data from reference [10], page 145.

Probit Equation
Total Destruction Probit = − 228.7 + 20.6 ℓn P

TABLE 3-11. EXPLOSION DAMAGE LEVELS FOR SPHERICAL TANK*

Target	Damage Level	Peak Overpressure	
		psi	(N/m^2)
Steel, spherical petroleum tank	(20%) Structural Damage	8.0	55,158
	(99%) Total Destruction	16.0	110,316

*Based on data from reference [10], page 145.

Probit Equation
Total Destruction Probit = − 45.8 + 4.6 ℓn P

32

Chapter 4

DOSE-RESPONSE ESTIMATES FOR
HYDROGEN FLUORIDE (HF) GAS AND MAN

GENERAL PROPERTIES

Hydrogen fluoride (HF) is a liquid or gas of boiling point about 19°C (67°F) which used to be transported in cylinders. Its physical properties are:

> Vapor pressure at 70°F -- 0.6 psig
> Liquid density at 0°C --- 1.003 g/ml
> Gas density at 34°C -- 1.27 (air = 1)
> Latent heat of vapor at boiling point -- 80.45 cal/g
> Specific heat of liquid at 20°C -- 0.61 cal/g °C

HF is very reactive, has a high affinity for water, fumes strongly in air (unless very dry), and the liquid reacts very vigorously with water.

Its general properties as a toxicant may be summed up as similar to HCl but more intense: i.e., a strong primary irritant, more aggressive than HCl, and also having more lasting and serious toxic effects.

The Threshold Limit Value (TLV) of hydrogen fluoride is 3 ppm (2 mg/m^3). Exposures to low concentrations above this, say 10 mg/m^3, are experienced as eye and respiratory irritation and acid taste. At about 100 mg/m^3 the limit of tolerance is about one minute, and this is clearly a hazardous concentration; however, as with other strong irritants, no one would voluntarily take a hazardous dose. At 100 mg/m^3 the skin also reacts, with rapid smarting and reddening; this does not occur at 50 mg/m^3.

Burns from liquid contact or high vapor concentration are very severe, extremely painful, and slow to heal. Ulceration is common (skin and respiratory tract) and gangrene may occur. First aid procedures emphasize very thorough washing of skin and eyes, neutralizing chemically, and anesthesia of eyes.

Respiratory exposure to high concentrations clearly presents a two-fold hazard: respiratory spasm from intolerable irritation, and later chemical pneumonia with edema. Treatment of casualties therefore requires absolute rest and administration of 100% oxygen.

DOSE-RESPONSE ESTIMATES

Higgins et al. [17] exposed rats and mice to hydrogen fluoride for five minutes at levels which killed some or all animals in most groups. Pulmonary edema was seen in most of the dead animals and pulmonary hemorrhage in those exposed above the LC_{50}. Delayed deaths were routinely observed below the LC_{50}, peaking at 24 hours but with some at three to four days after exposure.

Wohlslagel et al. [18] exposed rats and mice for 60 minutes, also at levels showing zero to 100% lethality. Signs during exposure included eye and mucous membrane irritation, respiratory distress, corneal opacity, and skin erythema. Rats dying during or after exposure showed pulmonary congestion, intra-alveolar edema and some thymic hemorrhage; mice showed pulmonary congestion and hemorrhage.

Both papers analyze results in terms of concentration and they report LC_{50} values. Concentration is, of course, directly proportional to dosage within each paper since a constant exposure time was used in each set of experiments, but the papers cannot be directly compared. We have converted exposures to dosages (concentration x time) and they are plotted in Figure 4-1. It will be seen that the 5-minute and 60-minute rat exposures gave approximately the same LCt_{50} and same slope. The 60-minute mouse exposures gave a similar slope but lower LCt_{50}. The 5-minute mouse exposures gave a less steep slope of lethality vs. dosage and a somewhat higher LCt_{50} than at 60 minutes. The combined mouse results clearly give a less satisfactory interpretation. We use the rat and 5-minute mouse results in the following discussion.

Both groups of investigators also exposed animals to hydrogen chloride, and the rat results at 5-minute and 60-minute exposures can be similarly combined. The calculated LCt_{50} values are:

			$mg\ min\ m^{-3}$		
Higgins et al.	LCt_{50}	HCl	307,420	Ratio	5.1 : 1
	LCt_{50}	HF	60,665		
Wohlslagel et al.	LCt_{50}	HCl	281,160	Ratio	5.0 : 1
	LCt_{50}	HF	55,800		

[17] Higgins, E. A., V. Fiorica, A. A. Thomas, and H. V. Davis, Acute toxicity of brief exposures to hydrogen fluoride, hydrogen chloride, nitrogen dioxide and hydrogen cyanide with or without carbon monoxide, *Fire Technol.* 8(2):120-130, 1972.

[18] Wohlslagel, J., C. DePasquale, and E. H. Vernat, Toxicity of solid rocket motor exhaust: Effects of hydrogen chloride, hydrogen fluoride and alumina on rodents, *J. Combust. Toxicol.* 3(1):61-70, 1976.
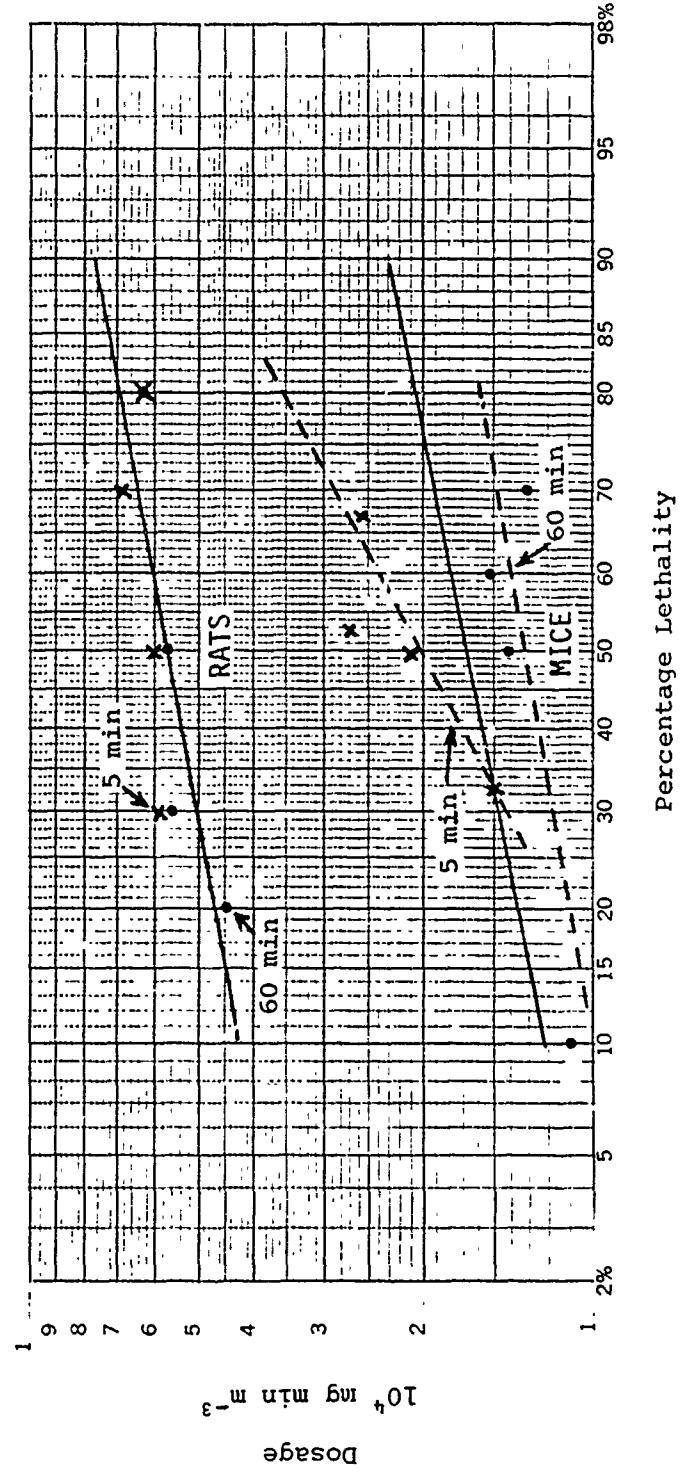
FIGURE 4-1. Hydrogen Fluoride Lethality

35

The two sets of figures are remarkably similar for the separate experiments.

These data are the best available to us and they support a dosage-dependent (Haber) approach for exposures of 5 to 60 minutes, a range that must include the large majority of exposures in any probable VM incident with HF. We can reasonably assume the same response slope for man, but the LCt_{50} is not so easy to estimate. Including the quoted papers, we have the following:

Time, min	Species	Conc., mg m^{-3}	Ct, mg min m^{-3}	Response	Reference
5	Rat	12,100	60,500	LCt_{50}	Higgins et al. [17]
30-60	Man	33	990-1980	May be fatal	Braker & Mossman [19]
60	Rat	930	55,800	LCt_{50}	Wohlslagel et al. [18]
60	Rat	850	51,000	LCt_{50}	Darmer et al. [20]
60	Mouse	228	13,680	LCt_{50}	Wohlslagel et al. [18]
60	Mouse	300	18,000	LCt_{50}	MacEwen & Vernot [21]

There are a few isolated figures for other species, but they do not help us.

It will be seen that the rat data are a reasonably consistent group and so are the mouse data at a lower level, but the estimate for man is conspicuously out of line. The basis for this estimate is not given by the source, and the concentration of 33 mg m^{-3} cannot be reconciled with the statement that 27 mg m^{-3} has been used for inhalation therapy of tuberculosis (ACGIH, [22]) nor with other response levels such as a one-minute toxic effects threshold of 73 mg m^{-3}. If we refer back to our earlier estimates for hydrogen chloride, we find that these support an LCt_{50} of approximately 40,000 mg min m^{-3} for man. Applying the fraction HF/HCl = 1/5 (see above), this gives an estimate for HF of 8,000 mg min m^{-3}

[19] Braker, W., and A. L. Mossman, *Effects of Exposure to Toxic Gases—First Aid and Medical Treatment,* Matheson Gas Products, East Rutherford, N.J., 1970.

[20] Darmer, K. I., Jr., C. C. Haun, and J. D. MacEwen, The acute inhalation toxicology of chlorine pentafluoride, *Am. Ind. Hyg. Assoc. J.* *33*:661, 1972.

[21] MacEwen, J. D., and E. H. Vernot, *Toxic Hazards Research Units Annual Technical Report,* TR-74-78, Aerospace Medical Research Laboratory, Wright-Patterson AFB, Dayton, Ohio, July 1974.

[22] American Conference of Governmental Industrial Hygienists, *Documentation of Threshold Limit Values for Substances in Workroom Air,* ACGIH, Cincinnati, Ohio, 1975.

which is more in line with the animal data. Our recommendation is to use an estimate of 10,000 mg min m^{-3} for the LCt$_{50}$ of HF for man, over the exposure time range of 5 to 60 minutes. This gives the following rough estimates for other levels of lethality:

	mg min m^{-3}
100%	20,000
95%	16,000
(50%)	(10,000)
5%	6,000
0	5,000

The resulting probit equation for lethality is:

$$Probit = -25.8689 + 3.3545 \, \ln Ct$$

It may be that the estimated LCt$_{50}$ is in error by twofold or more. This would put it outside the above range of response, but it should be noted that the whole of this range is quite narrow in comparison with the very wide range of exposures likely to be experienced in a VM inci- dent. If exposures are such that the spectrum of response extends from massive overkill to far below the lethal threshold, a twofold error in LCt$_{50}$ estimates will affect the fate of only a small part of the whole population and the casualty estimate will be in error by much less than twofold.

There is some support for the chosen numerical range in that the lowest concentrations at the threshold of lethality (i.e., at the longest exposure times) are about 100 mg m^{-3}:

	mg min m^{-3}	mg m^{-3} for 60 min
LCt$_5$	6,000	100
(max) LCt$_0$	5,000	83

This is a concentration that is stated to be the highest tolerable for one minute, reactions including eye and mucous irritation, skin red- dening, and sour taste (Patty, [23]). Longer exposure than one minute would be immediately incapacitating, and it might be expected that a few deaths would occur (later) in those exposed for 30 to 60 minutes.

The sublethal zone presents a difficult problem because of the very scanty information. In addition to the 100 mg m^{-2} threshold just cited, it is said that 50 mg m^{-3} has similar effects without skin reaction and that 26 mg m^{-3} is tolerated "for several minutes" (Patty, [23]). The

---

[23] Patty, F. A. (ed.), *Industrial Hygiene and Toxicology*, Interscience Publishers, New York, 1962.

threshold for toxic effect (irritation) is given as 21 mg m^{-3} (Christensen, [24]), and there is sensory response below this level. The TLV is 2 mg m^{-3}. We accordingly suggest (very tentatively) the following for 5- to 60-minute exposure:

Conc., mg m^{-3}	Response
25 - 100	Temporary incapacitation
5 - 25	Harassment
0 - 5	Zero

As a result, we retain the probit equation for injury based on HCl:

$$\text{Probit} = 2.7967 + 2.90 \ln Ct$$

[24] Christensen, H. E., et al. (eds.), *Registry of Toxic Effects of Chemical Substances*, U.S. Department of Health, Education and Welfare, NIOSH, Rockville, Md., 1976.

Chapter 5

SIMPLIFICATION OF USER INPUT DATA

DATA REQUIREMENTS

To run the VM, the user is required to prepare a user input file. A list of variables needed for this is contained in Table B.1 of the *Vulnerability Model User's Guide,* and reproduced here as Tables 5-1a and 5-2. These variables can be divided into six categories. The data in the 1000 series are mainly the physical properties of the spilled chemical, which are accessed from the chemical properties file during execution. In principle, this file contains 74 physical and chemical properties for each chemical. However, in practice, many of the properties are not available for the chemicals. For this reason, we prefer to prepare the chemical property variables by means of the user input file. The user's input is always given a higher source code than default or other values; it takes precedence in the program to ensure that the right chemical properties are used in the VM execution.

The 2000 series includes data of the tank, cargo, and environment which must be supplied by the user. Though there are default values for all the state variables, some of the default values are far from the actual spill situation and will cause incorrect results.

There are only a few variables in the 3000 series. The 4000 and 5000 series variables are mainly for fire, explosion, and toxicity. Some of the variables can be read from the chemical properties file.

The 6000 series are variables concerning computing time-steps and the location of the spill. The spill location is specified by its longitude and latitude. The user has to be very careful in filling these data, because one minute difference in longitude will move the location about one mile away.

Once the user input file, chemical properties file, and default file have been accessed and the VM data base is complete, these variables along with their source codes are stored on a temporary file named the state file.

There are about 170 state file variables; however, not all of these variables are used at one time for a given problem. Selecting the necessary state variables for a problem is often difficult. To help the user in doing this, we have made input samples for several hazardous chemicals which are frequently transported in large quantities. Should there be a spill of one of these chemicals, the user can prepare the input by following the sample sheet of the pertinent chemical and substituting the required values according to the current accident situa-

tion. The samples are listed for LNG, chlorine, ammonia, hydrogen
fluoride, methyl bromide, hydrogen chloride, and methanol (Tables 5-1a
through 5-1g, respectively).

Explanation of the sample LNG sheet (Table 5-1a) is as follows:

- Name the state file just as in ordinary program.

- The code numbers, such as 1001, 1002, etc., are four
  digits and start in column 1.

- The first datum is the chemical name in code which has
  to start in column 5. All other data except the first
  one start in column 6. If the numerical value is
  negative, the minus sign is in column 6.

- If the numerical value is expressed in exponential form,
  it should be written as .4321E+07 or 4.321E+06 or
  43210E+02. There are five digits or four digits and
  a decimal point before the character E, no more and no
  less.

- After the last line of data there should be at least
  one blank line; otherwise the program will stop to
  execute and print out "--end of file--".

- The "Unit" and "Description" columns in Table 5-1a are for
  reference only. Do not write them in the input.

- Table 5-2 lists all flags used in VM.

TABLE 5-1a. LNG SAMPLE INPUT

Input COLUMN NUMBER		Unit	Description
1 0 0 1 L N G			
1 0 0 2 1 6 . 0 4		gm/mol	Molecular weight, typical value
2 0 0 1 2 . 0 0 0 E 0 8		cm³	Tank volume
2 0 0 2 5 0 0 . 0		cm	Tank height
2 0 0 3 1 0 0 . 0		cm	Hole height
2 0 0 4 − 1 5 1 . 0		°C	Tank temperature before discharge
2 0 0 5 2 . 0 2 7 E 0 6		dyne/cm²	Tank pressure before discharge
2 0 0 6 1			(See Table 5-2)
2 0 0 7 8 . 3 0 0 E 0 7		gm	Initial mass
2 0 0 8 5 0 .		cm	Diameter of hole
2 0 1 4 1 0 0 . 0		cm	Coordinate z, above ground
2 0 1 5 0 .		cm	Height of center of hole, above water
2 0 1 6 4 0 0 . 0		cm/sec	Wind speed
2 0 1 7			Flag; see Table 5-2
2 0 1 8			Flag; see Table 5-2
2 0 1 9		cm	Length of channel, if 2018=1; radius of pool, if 2018=2
2 0 2 0 6 . 0 9 6 E 0 4		cm	Channel width
2 0 2 1 1 . 2 4 6 E − 0 4		gm/cc	Hazard concentration
2 0 2 2 1			Flag; see Table 5-2
2 0 2 3 2 0 . 0		°C	Water temperature
2 0 2 5 1			Flag; see Table 5-2
2 0 2 7 1 8 0 . 0		sec	Evaporation time
2 0 5 8 1 0 . 0		deg	Wind direction
3 0 0 4 1			Flag; see Table 5-2
3 0 0 6 2			Shielding situation; see Table 5-2

(continued)

41

TABLE 5-1a (continued). LNG SAMPLE INPUT

Input		Unit	Description
COLUMN NUMBER 1 — 5 6 7 10 15			
5 0 0 1	0		Flag; see Table 5-2
5 0 0 2	0		Flag; see Table 5-2
5 0 0 3	1		Flag; see Table 5-2
5 0 0 4	0		Flag; see Table 5-2
5 0 1 0	0		Flag; see Table 5-2
5 0 1 1	1 . 0	gm/cc	Density of water
5 0 1 2	- 1 8 2 . 0	°C	Freezing point of chemical
5 0 1 3	5 . 4	--	Lower inflammability limit, percent concentration
5 0 1 4	1 4 .	--	Upper inflammability limit, percent concentration
5 0 1 6	- 1 . 3 0 E 0 4		Heat of combustion
5 0 1 7	1 8 7 5 .	°C	Adiabatic flame temperature
5 0 1 8	2 . 0 8 3 E - 0 2	cal/gm	Burning rate of chemical
5 0 1 9	2 .	--	Mole of oxygen per mole of fuel
5 0 2 0	- 1 6 1 . 0	°C	Flash point of chemical
5 0 2 1	1 . 4	--	Ratio of specific heat
5 0 2 2	1 . 0 1 3 E - 0 6	dyne/cm^2	Ambient atmosphere pressure
5 0 3 8	. 5	--	Fraction of population sheltered
6 0 0 1	0 .	sec	Time, begin loop 1
6 0 0 2	0 .	sec	Time, end loop 1
6 0 0 3	0 .	sec	Time increment value of loop 1
6 0 0 4	1 . 0	min	Time, begin loop 2
6 0 0 5	1 5 .	min	Time, end loop 2
6 0 0 6	1 .	min	Time increment of loop 2
6 0 0 7	0	min	Time, begin loop 3
6 0 0 8	0	min	Time, end loop 3
6 0 0 9	0	min	Time increment of loop 3
6 0 1 0	2 9 5 8 0 0 .	--	Latitude, north of spill site, 29°58'00"
6 0 1 1	9 0 0 9 0 0 .	--	Longitude, west of spill site, 90°09'00"

42

TABLE 5-1b	TABLE 5-1c	TABLE 5-1d
INPUT FILE OF CHLORINE	INPUT FILE OF AMMONIA	INPUT FILE OF HYDROGEN FLUORIDE

```
Chlorine Spill

1001CLX
2001 .1000E+08
2002 500.0
2003 0.0
2004 -33.90
2005 .1013E+07
2006 0.
2007 .1500E+08
2008 50.00
2016 400.0
2017 4.000
2121 .2980E-05
2023 15.00
2036 -33.90
2058 53.00
3004 1.000
3006 25.00
3002 0.
3008 1.000
3007 0.
5001 0.
5002 0.
5003 1.000
5004 1.000
5010 0.
5011 1.000
5012 -101.0
5021 1.400
5022 .1013E+07
5030 2.750
5031 -17.10
5032 1.690
5033 -2.400
5034 2.900
5035 3.000
5036 .1000E-06
5037 0.
5038 .5000
6001 0.
6002 0.
6003 0.
6004 2.000
6005 30.00
6006 2.000
6007 0.
6008 0.
6009 0.
6010 .2958E+06
6011 .9015E+06
   0 0.
```

```
Ammonia Spill

1001AMA
2001 .3100E+08
1002 17.03
1004 .6821
2044 500.0
2047 100.0
2045 1000.
2002 500.0
2003 0.
2004 21.00
2005 .8800E+07
2006 0.
2007 .3100E+08
2008 15.24
2016 600.0
2123 15.00
2027 2400.
2029 1.000
2038 8818.
2036 21.00
2054 -9.000
2058 53.00
3004 0.
3006 3.000
3002 0.
3008 1.000
3007 0.
4001 .2120E+08
4004 2400.
5001 0.
5002 0.
5003 1.000
5004 1.000
5010 1.000
5011 1.000
5012 -101.0
5021 1.400
5022 .1013E+07
5030 2.750
5031 -30.57
5032 1.385
5033 0.
5034 0.
5035 100.0
5037 0.
5038 .5000
6001 0.
6002 0.
6003 0.
6004 2.000
6005 40.00
6006 2.000
6007 0.
6008 0.
6009 0.
6010 .2958E+06
6011 .9015E+06
   0 0.
```

```
Hydrogen
Fluoride
Spill

1001HFA
1002 20.006
1003 19.5
1004 1.003
1006 .2560E-02
1007 .61
1008 10.1
1013 3.0
1009 .00317
1014 80.45
1021 1.003
2001 2.400E+08
2002 347.5
2003 0.
2004 21.0
2005 .1013E+07
2006 0.
2007 2.000E+08
2008 15.24
2016 400.0
2017 2.
2023 29.5
2025 1.
2028 1.
2029 1.
2036 21.
2044 500.
2047 100.
2054 25.0
2058 53.0
3002 0.
3004 0.
3006 3.
4002 1.500E+08
4003 1.490E+08
5001 0.
5002 0.
5003 1.
5004 1.
5010 0.
5001 1.
5012 -83.37
5030 2.75
5031 -14.0719
5032 1.69
5033 2.79663
5034 2.9
5035 2.0
5038 0.5
6001 0.
6002 0.
6003 0.
6004 2.
6005 30.
6006 2.
6007 0.
6008 0.
6009 0.
6010 295800.
6011 901500.
   0 0.
```

TABLE 5-1e	TABLE 5-1f	TABLE 5-1g
INPUT FILE OF METHYL BROMIDE	INPUT FILE OF HYDROGEN CHLORIDE	INPUT FILE OF METHANOL

```
Methyl
Bromide
Spill

1001MTB
1002 94.944
1003 3.56
1004 1.730
1006 .3970E-02
1007 .197
1013 .1106
1009 .3170E-02
1014 60.23
1021 1.730
2001 2.400E+08
2002 347.5
2003 0.
2004 21.0
2005 .1013E+07
2006 0.
2007 4.000E+08
2008 15.24
2016 400.0
2017 2.
2023 29.50
2025 1.
2027 2400.
2028 1.
2029 1.
2036 21.
2044 500.
2047 100.
2054 25.0
2058 53.0
3002 0.
3004 0.
3006 3.
4002 2.500E+08
4003 .1445E+09
5001 0.
5002 0.
5003 1.
5004 1.
5010 0.
5011 1.
5012 -93.7
5030 2.75
5031 -19.9241
5032 5.1565
5033 0.
5034 0.
5035 9.0
5038 0.5
6001 0.
6002 0.
6003 0.
6004 2.
6005 30.
6006 2.
6007 0.
6008 0.
6009 0.
6010 295800.
6011 901500.
   0 0.
```

```
Hydrogen
Chloride
Spill

1001HDC
1002 36.461
1003 -85.03
1004 1.194
1005 .2560E-02
1008 24.72
1013 .1939
1009 .001639
1014 103.12
1021 1.194
2001 2.400E+08
2002 347.5
2003 0.
2004 085.03
2005 .1013E+07
2006 0.
2007 2.600E+08
2008 15.24
2016 400.0
2017 2.
2023 29.5
2025 1.
2027 2400.
2028 1.
2029 1.
2036 21.
2044 500.
2047 100.
2054 25.0
2058 53.0
3002 0.
3004 0.
3006 3.
4002 1.800E+08
4003 .1500E+09
5001 0.
5002 0.
5003 1.
5004 1.
5010 0.
5011 1.
5012 -114.19
5030 2.75
5031 -21.7631
5032 2.6518
5033 0.
5034 0.
5035 3.0
5038 0.5
6001 0.
6002 0.
6003 0.
6004 2.
6005 30.
6006 2.
6007 0.
6008 0.
6009 0.
6010 295800.
6011 901500.
   0 0.
```

```
Methanol Spill

1001MAL
2001 1.300E+09
2002 1600.0
2003 0.0
2004 15.0
2005 1.013E+06
2006 0.0
2007 1.000E+09
2008 100.
2016 670.6
2017 1.
2023 20.
2054 25.
2058 55.
3004 1.0
3006 1.0
5002 1.
5003 1.0
5004 1.0
5036 .001
6001 10.0
6002 20.0
6003 10.0
5006 2.
2028 1.0
2029 0.0
5019 1.5
2043 .0000156
5005 .001
6010 295625.
6011 900330.
   0 0.
```

44

TABLE 5-2. STATE FILE VARIABLES - FLAGS

Field Number	Variable	Default Value	Description
2006	IADBI	1	For tank condition: =0, isothermal; =1, adiabatic (MODA)
2017	IAC	6	Atmosphere condition: =1, extremely unstable; =2, moderately unstable; =3, slightly unstable; =4, neutral; =5, slightly stable; =6, moderately stable
2018	IDIM	2	For spill: =1, channel spill; =2, radial spill (MODD)
2022	IQ	1	Conditions of heat transfer from water to chemical: =1, constant; =2, limited by ice formation (MODD)
2025	ITC	1	=1, to calculate critical values (MODD)
2028	IFLAG	1	Spill environment: =1, for still water; =2, flowing water; =3, tidal water (MODP)
2029	ICOND	0	Duration of discharge: =0, short duration; =1, continuous discharge
3004	NSF	0	Secondary source flag: =0, no, =1, yes
3005	ISF	0	Number of secondary sources
3006	ISHLD	3	Shielding situation: =1, maximum; =2, minimum; =3, intermediate
5001	MFLAG	0	Output message: =0, no message; =1, message for each state file variable stored; =2, message for each state file variable retrieved; =3, message for each state file variable stored or retrieved
5002	J5002	0	Miscibility of chemical in water: =0, no; =1, yes
5003	J5003	0	Inflammability of chemical =0, no; =1, yes
5004	ITOX	0	Toxicity of chemical: =0, no; =1, yes
5005	IWAT	0	Liquid toxicity: =0, no; =1, yes
5006	IIGN	0	Type of ignition: =0, no ignition; =1, flash fire; =2, flash fire and pool burning; =-1, explosion; =-2, explosion and pool burning
5010	ISCS	0	=0, use puff equation; =1, use plume equation (MODZ)

VM EXECUTION

At the present time the Vulnerability Model resides on the CDC CYBER 70 series computer in Rockville. The source programs are stored in a program library on the SCOPE batch system; the Chemical Properties file, Default file, and DPI file are stored on magnetic tape storage on SCOPE; and an interactive procedure, designed to execute the VM with user-specified data bases, resides on the NOS time-sharing system.

This interactive procedure, called P34, allows the user who may be unfamiliar with the CDC operating system to run the VM with different spill locations and parameters. By invoking P34, the user is prompted for the names of several data bases which have previously been stored on the NOS system:

(1) The user data containing the spill parameters and tank and atmospheric conditions.

(2) The Geographic file containing the vulnerable resources data.

(3) The Secondary Source file containing the type, location, and physical parameters of the secondary fire sources.

(4) The Source Modification file containing FORTRAN source modifications to the VM (the user is not prompted for the name of this file if no modifications are being tested or made).

The user is also queried for the type of run (full, part, or executive) and whether he wants to change any of the default run parameters.

Following these prompts, P34 routes the completed job to SCOPE at which time the VM is run. The output from this run is returned to the user's batch printer.

A complete description of P34 has been made available to USCG personnel [25].

---

[25] Control Data Corporation, *SCOPE 3.4-NOS Version of Enviro Control's Vulnerability Model*, October 1976.

46